analytical chemistry

Article

Cite This: *Anal. Chem.* XXXX, XXX, XXX−XXX

pubs.acs.org/ac

# Use of a Phosphatase-Like DT-Diaphorase Label for the Detection of Outer Membrane Vesicles

Andi Muhammad Ichzan, Sohee Lee, Chiew San Fang, Ponnusamy Nandhakumar, Hyeri Ha, Jung Min Joo, Kwang-sun Kim,* and Haesik Yang*

Department of Chemistry and Chemistry Institute for Functional Materials, Pusan National University, Busan 46241, Korea

Supporting Information

**ABSTRACT:** DT-diaphorase (DT-D) is known to mainly catalyze the two-electron reduction of quinones and nitro(so) compounds. Detection of Gram-negative bacterial outer membrane vesicles (OMVs) that contain pyrogenic lipopolysaccharides (LPSs, also called endotoxins) is required for evaluating the toxic effects of analytical samples. Here, we report that DT-D has a high dephosphorylation activity: DT-D catalyzes reductive dephosphorylation of a phosphate-containing substrate in the presence of NADH. We also report that sensitive and simple OMV detection is possible with a sandwich-type electrochemical immunosensor using DT-D and two identical LPS-binding antibodies as a catalytic label and two sandwich probes, respectively. The absorbance change in a solution containing 4-nitrophenyl phosphate indicates that dephosphorylation occurs in the presence of both DT-D and NADH. Among the three phosphate-containing substrates [4-aminophenyl phosphate, ascorbic acid phosphate, and 1-amino-2-naphthyl phosphate (ANP)] that can be converted into electrochemically active products after dephosphorylation, ANP shows the highest electrochemical signal-to-background ratio, because (i) the dephosphorylation of ANP by DT-D is fast, (ii) the electrochemical oxidation of the dephosphorylated product (1-amino-2-naphthol, AN) is rapid, even at a bare indium−tin oxide electrode, and (iii) two redox cycling processes significantly increase the electrochemical signal. The two redox cycling processes include an electrochemical−enzymatic redox cycling and an electrochemical−chemical redox cycling. The electrochemical signal in a neutral buffer (tris buffer, pH 7.5) is comparable to that in a basic buffer (tris buffer, pH 9.5). When the immunosensor is applied to the detection of OMV from *Escherichia coli*, the detection limit is found to be 8 ng/mL. This detection strategy is highly promising for the detection of biomaterials, including other extracellular vesicles.

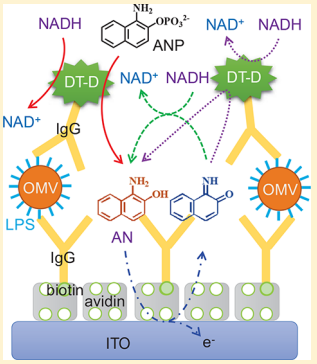


Outer membrane vesicles (OMVs, ∼50−250 nm in diameter) that are released from living bacteria and fungi play a role as tiny but effective cargo carriers that deliver proteins, lipids, and nucleic acids. The carriers are involved in the mediation of intercellular communication, the elimination of unwanted components, the modulation of host immune responses, and the promotion of virulence.[1−4] OMVs derived from Gram-negative bacteria, just like the bacteria themselves, can modulate undesired immune responses such as fever and septic shock, as pyrogenic lipopolysaccharides (LPSs, also called endotoxins) are present in their outer membranes.[5] In fact, the lipid A of LPS present in the outer membrane is responsible for the immune responses: LPSs become immunologically toxic when they are released from the outer membranes of bacteria and OMVs.[6,7] In the case of bacteria, it has been known that free LPSs are generated during cell growth and division and after cell death.[7,8] Importantly, in the case of OMVs, free LPSs are generated inside cytosol after OMVs enter the host cells by endocytosis.[9,10] The generation process of free LPSs by OMVs is very efficient for the delivery of toxic LPSs. Moreover, OMVs are stable and are released in larger numbers, even under the conditions that cause bacterial death, such as ultraviolet radiation.[11] This indicates that OMVs are promising biomarkers for evaluating the LPS-mediated toxicity independent of bacterial damage. Therefore, sensitive and accurate detection of the LPS amount from Gram-negative bacterial OMVs is required for evaluating possible toxic effects of analytical samples. While LPS detection has been widely studied, OMV detection has been rarely investigated.

The most common method for LPS detection is the limulus amebocyte lysate (LAL) test that is based on LPS-induced proteolytic cascade reactions and resulting gel-clot formation. However, the test is limited by protease interference, lot-to-lot variation, and finite resources of the test reagents.[5,12] To overcome these limitations, various affinity assays have been developed that use LPS-binding proteins/peptides, antibodies, and aptamers.[5,12−15] Most of the assays are based on single affinity binding, which limits sensitive and accurate LPS detection. Affinity assays are also suitable for OMV detection, because it is difficult to accurately determine the size and concentration of OMVs even after OMVs are fully isolated from a sample. One OMV contains many LPSs in its outer membrane,[1,12−15] which might facilitate the detection of OMV by a sandwich-type immunoassay using double affinity binding

**Received:** January 5, 2019
**Accepted:** February 21, 2019






DOI: 10.1021/acs.analchem.9b00064
*Anal. Chem.* XXXX, XXX, XXX−XXX

of two identical anti-LPS antibodies. However, to date, this sandwich-type OMV detection has not been reported.

In living organisms, phosphorylation and dephosphorylation are required for energy storage/release, enzyme activation/deactivation, and catabolism.[16−18] Many kinases and phosphatases are involved in these reactions. Because dephosphorylation by alkaline phosphatase (ALP) is very fast, ALP is commonly used as a catalytic label in biosensors.[19−21] Some redox enzymes, such as dehydrogenases, can also be involved in the reversible oxidative phosphorylation, using $NAD^+$ as an oxidant.[22−24] Its reverse reaction corresponds to the reductive dephosphorylation using NADH as a reductant. NAD(P)H dehydrogenase (quinone) [DT-diaphorase (DT-D)] is a redox enzyme that catalyzes the two-electron reduction of quinones by using NADH or NADPH as a reductant. DT-D from *Bacillus stearothermophilus* (EC 1.6.99.-) has been used as a catalytic label in biosensors to obtain high and reproducible signal amplification because of its high catalytic activity and thermal stability. DT-D also allows fast catalytic reduction of nitro and nitroso groups and fast electrochemical−enzymatic (EN) redox cycling in the presence of NADH.

Here, we report an electrochemical sandwich-type immunosensor for the sensitive and simple detection of OMVs, based on the reductive dephosphorylation of a phosphate-containing substrate by DT-D in the presence of NADH. The dephosphorylated product participates in EN and electrochemical−chemical (EC) redox cycling. First, the phosphatase-like activity of DT-D was investigated with dephosphorylation of 4-nitrophenyl phosphate (NPP). Three phosphate-containing substrates [4-aminophenyl phosphate (APP), ascorbic acid phosphate (AAP), and 1-amino-2-naphthyl phosphate (ANP; Figure 1a)] that are converted into electrochemically active

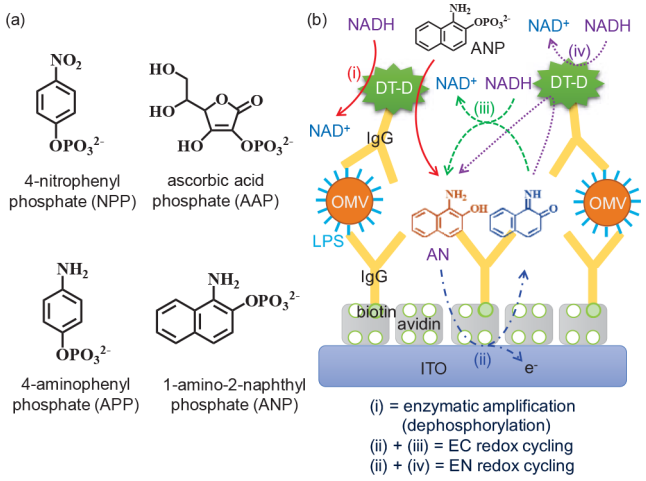


**Figure 1.** (a) Phosphate-containing substrates and (b) schematic of a sandwich-type electrochemical immunosensor for OMV detection.

products after dephosphorylation were compared in terms of electrochemical signal-to-background ratio. Finally, the immunosensor was applied to the detection of OMVs isolated from *Escherichia coli* (*E. coli*; Figure 1b), and its detection limit was determined.

## EXPERIMENTAL SECTION

**Chemicals and Solutions.** DT-D from *Bacillus stearothermophilus* (EC 1.6.99.-) and diaphorase (EC 1.8.1.4) were obtained from Nipro Co. (Osaka, Japan). *E. coli* BW 25113 strain was obtained from the Coli Genetic Stock Center (CGSC; strain 7636). ALP, nitroreductase from *E. coli* (N9284), hydroxylamine hydrochloride, $H_2O_2$, $NH_4OH$, sodium hydroxide, ethylenediaminetetraacetic acid, NADH (*β*-nicotinamide adenine dinucleotide reduced dipotassium salt), NPP disodium salt, 4-nitrophenol (NP), bovine serum albumin (BSA), and all the reagents used for the preparation of buffer solutions were purchased from Sigma−Aldrich Co. Anti-*E. coli* LPS IgG was obtained from Abcam (ab35654, Cambridge, U.K.). Sulfosuccinimidyl-6-[biotinamido]-6-hexanamidohexanoate (EZ-link sulfo-NHS-LC-LC-biotin), sulfosuccinimidyl-4-[*N*-maleimidomethyl]cyclohexane-1-carboxylate (sulfo-SMCC), *N*-succinimidyl-*S*-acetylthiopropionate (SATP), and Pierce BCA protein assay kit were obtained from Thermo Scientific Inc. (Rockford, IL, U.S.A.). ANP was synthesized as previously reported.[25] 1-Amino-2-naphthol (AN) was obtained from TCI (Tokyo, Japan), and AAP magnesium salt hydrate was obtained from Wako Pure Chemical Industries, Ltd. (Osaka, Japan). Luria−Bertani broth (LB) media was obtained from Difco (244620, Sparks, MD, U.S.A.).

Phosphate-buffered saline (PBS, pH 7.4) contained 10 mM phosphate, 0.138 M NaCl, and 2.7 mM KCl. Phosphate-buffered saline with BSA (PBSB) contained all the ingredients in PBS along with 1% (w/v) BSA. Tris buffers (pH 9.5 and 7.5) were prepared using 50 mM tris and 1.0 M HCl. The rinsing buffer (pH 7.6) contained 50 mM tris, 40 mM HCl, 0.05% (w/v) BSA, 0.05% Tween 20, and 0.5 M NaCl. Indium tin oxide (ITO) electrodes were purchased from Corning Co. (Daegu, Korea).

**Conjugation Procedure.** DT-D-conjugated anti-LPS IgG was prepared by cross-linking the amine group of anti-LPS IgG and the amine group of DT-D. A total of 1 mL of PBS containing 100 *μ*g/mL anti-LPS IgG and 10 *μ*L of PBS containing 2 mg/mL SATP were mixed for 30 min at 22 ± 2 °C. Afterward, the solution was mixed with 20 *μ*L of a deacetylation solution containing 0.012 g/mL ethylenediaminetetraacetic acid and 0.044 g/mL hydroxylamine hydrochloride for 2 h at 22 ± 2 °C, and the SATP-modified anti-LPS IgG was filtered via centrifugation for 20 min at 12000 rpm. The filtrate was dissolved in 1 mL of PBS. A total of 1 mL of PBS containing 100 *μ*g/mL DT-D and 50 *μ*L of PBS containing 1 mg/mL sulfo-SMCC were mixed and incubated for 30 min at 22 ± 2 °C. Sulfo-SMCC-modified DT-D was filtered via centrifugation for 20 min at 12000 rpm. A 1 mL aliquot of PBS containing 100 *μ*g/mL SATP-modified anti-LPS IgG was then mixed with 1 mL of PBS containing 100 *μ*g/mL sulfo-SMCC-modified DT-D at a molar ratio of 1:1, and the mixture was incubated for 2 h at 22 ± 2 °C. The mixture was then centrifuged for 20 min at 12000 rpm to filter the DT-D-conjugated anti-LPS IgG. The filtrate was dissolved in 1 mL of PBSB.

Biotinylated anti-LPS IgG was obtained by cross-linking EZ-link sulfo-NHS-LC-LC-biotin and the amine group of anti-LPS IgG. A total of 1.33 *μ*L of 10 mM EZ-link sulfo-NHS-LC-LC-biotin and 1 mL of PBS containing 100 *μ*g/mL anti-LPS IgG were mixed and incubated for 2 h at 4 °C. The mixture was centrifuged for 20 min at 12,000 rpm to filter biotinylated anti-LPS IgG. The filtrate was dissolved in 1 mL of PBSB. Amicon Ultra centrifugal filter units (0.5 mL; 10K and 50K) from Merck Millipore Ltd. were used for the centrifugal filtering.

**OMV Preparation and Analysis.** *E. coli* BW25113 strain was cultured to an optical density ($OD_{600}$) of 3.0 at 37 °C in


DOI: 10.1021/acs.analchem.9b00064
Anal. Chem. XXXX, XXX, XXX−XXX

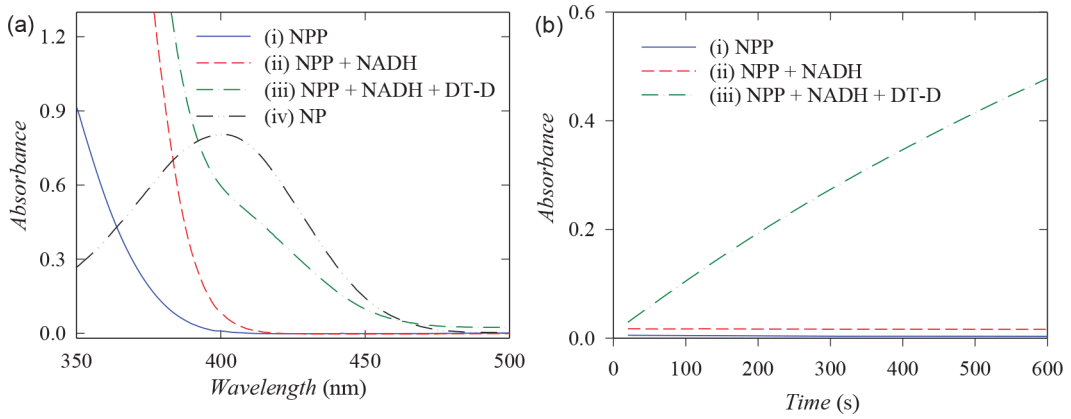


**Figure 2.** (a) Absorption spectra obtained after an incubation period of 10 min at 25 °C in tris buffer (pH 9.5) containing (i) 30 $\mu$M NPP, (ii) 30 $\mu$M NPP and 1.0 mM NADH, (iii) 30 $\mu$M NPP, 1.0 mM NADH, and 100 $\mu$g/mL DT-D, and (iv) 30 $\mu$M NP. (b) Time-course data of absorbance at 410 nm at 25 °C in tris buffer (pH 9.5) containing (i) 30 $\mu$M NPP, (ii) 30 $\mu$M NPP and 1.0 mM NADH, and (iii) 30 $\mu$M NPP, 1.0 mM NADH, and 100 $\mu$g/mL DT-D.

LB broth. OMVs were purified from bacterial culture medium, as described[26] from the filtered bacterial culture medium using a 0.22-$\mu$m syringe filter (BioFACT Co. Ltd., Daejeon, Korea) to make sure that OMV samples were completely separated from the *E. coli* cell culture medium. The OMV concentration was measured using a BCA protein assay kit. The purified OMVs were characterized by transmission electron microscopy (TEM) and nanoparticle tracking analysis (NTA). TEM and NTA were performed using JEM 1011 electron microscope (JEOL) and NanoSight LM10 (Malvern Panalytical Ltd., Worcestershire, U.K.), respectively, as described.[26,27] The OMV size was analyzed by NanoSight NTA software (v2.3.5.00).

**Preparation of Sensing Electrodes.** ITO electrodes were pretreated with a 5:1:1 solution of $H_2O$, $H_2O_2$ (30%), and $NH_4OH$ (30%) at 70 °C for 1 h.[28] To obtain avidin-modified ITO electrodes (avidin/ITO electrodes), 70 $\mu$L of carbonate buffer solution (20 mM, pH 9.6) containing 10 $\mu$g/mL avidin was dropped onto the ITO electrodes and incubated for 2 h at 20 °C. A total of 70 $\mu$L of PBSB containing 10 $\mu$g/mL biotinylated anti-LPS IgG were dropped onto the avidin/ITO electrodes and incubated for 30 min at 4 °C to obtain anti-LPS IgG/avidin/ITO electrodes. The surface of these electrodes was then treated with 70 $\mu$L of PBSB and incubated for 30 min at 4 °C to reduce nonspecific binding.

**Procedure of OMV Detection.** A total of 70 $\mu$L of PBS (or LB media sample) containing different concentrations of OMV was dropped onto a sensing electrode and incubated for 30 min at 4 °C. Next, 70 $\mu$L of PBSB containing 10 $\mu$g/mL DT-D-conjugated anti-LPS IgG was dropped onto the electrodes and incubated for 30 min at 4 °C, followed by washing with rinsing buffer. A total of 1 mL of tris buffer (pH 9.5) containing 1.0 mM NADH and 0.1 mM ANP was injected into an electrochemical cell that consisted of the immunosensing electrode, an Ag/AgCl (3 M NaCl) reference electrode, and a platinum counter electrode. The exposed geometric area of the immunosensing electrode was approximately 0.28 $cm^2$. Cyclic voltammetry and chronocoulometry were performed using CHI 1040C system (CH instruments, Austin, TX, U.S.A.).

## RESULTS AND DISCUSSION

**Absorbance Measurement for Dephosphorylation by DT-D.** To investigate dephosphorylation by DT-D, absorption spectra of a chromogenic substrate (NPP) were measured in four representative solutions (Figure 2a). In the presence of only NPP, the absorbance was almost 0 at wavelengths longer than 415 nm (curve i of Figure 2a). In the presence of NPP and NADH, the absorbance was high at wavelengths shorter than 415 nm (curve ii of Figure 2a) as the absorption by NADH is high in this region.[29] In the presence of NPP, NADH, and DT-D, the absorbance increased in the whole given range of wavelengths (curve iii of Figure 2a). The product (NP) formed after the dephosphorylation of NPP has an absorbance maximum around 400 nm (curve iv of Figure 2a). Therefore, the increased absorbance in the presence of NPP, NADH, and DT-D was due to the generation of NP by dephosphorylation of NPP.

Time-course absorbance data were also measured at 410 nm to check whether the absorbance changes with time in these three solutions. In the presence of NPP, the absorbance did not change with time (curve i of Figure 2b). In the presence of NPP and NADH, the absorbance also did not change (curve ii of Figure 2b). However, in the presence of NPP, NADH, and DT-D, the absorbance increased with time. It is clear that the dephosphorylation of NPP occurred in the presence of NADH and DT-D and that the reaction did not occur in their absence.

**Selection of a Phosphate Group-Containing Substrate.** High signal-to-background ratios are essential for sensitive detection, that is, the background levels should be low, whereas signal levels should be high. To obtain a low background level in Figure 1b, the substrate containing a phosphate group should be electrochemically inactive, and the electrochemical oxidation of NADH should be slow. To obtain a high signal level, the substrate should be rapidly converted to a dephosphorylated product by DT-D and NADH, and the product should be rapidly oxidized electrochemically at low potentials. To further increase the signal level, fast redox cycling should occur, that is, the oxidized form of the product should be rapidly reduced by DT-D and NADH.

As NADH is a strong reductant, it can be readily oxidized at metal and carbon electrodes. However, when low electrocatalytic ITO electrodes are used, NADH oxidation can be minimized up to 0.4 V.[30] Moreover, capacitive nonfaradaic


DOI: 10.1021/acs.analchem.9b00064
*Anal. Chem.* XXXX, XXX, XXX−XXX

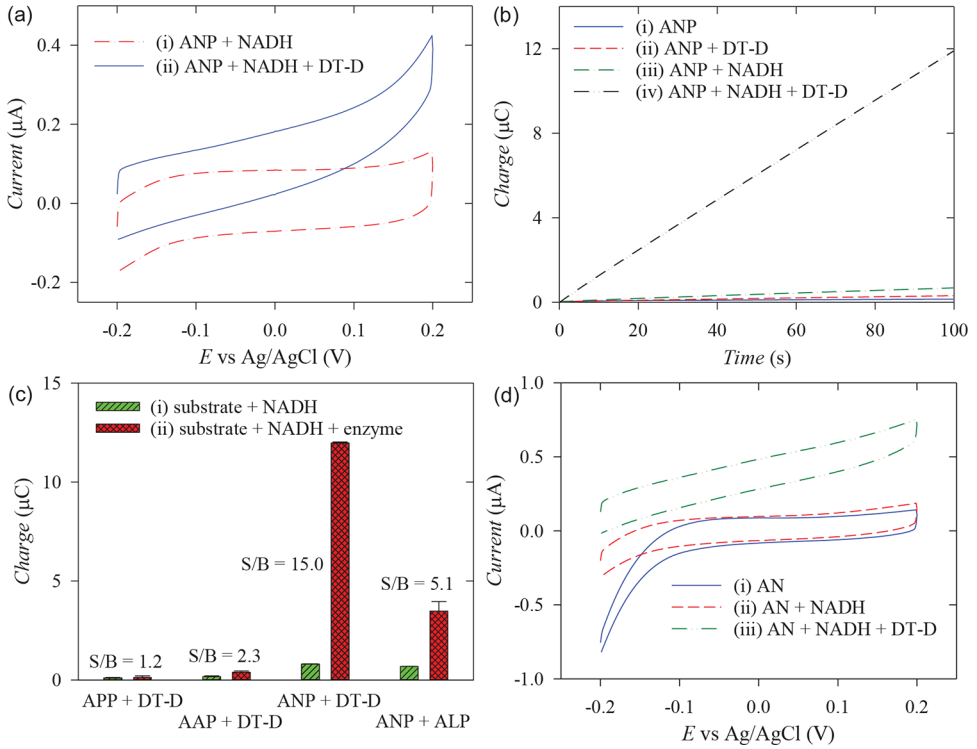


**Figure 3.** (a) Cyclic voltammograms obtained (at a scan rate of 20 mV/s) at bare ITO electrodes in tris buffer (pH 9.5) containing (i) 0.1 mM ANP and 1.0 mM NADH, and (ii) 0.1 mM ANP, 1.0 mM NADH, and 1 μg/mL DT-D after an incubation period of 10 min at 25 °C. (b) Chronocoulograms obtained at 0.10 V at bare ITO electrodes in tris buffer (pH 9.5) containing (i) 0.1 mM ANP, (ii) 0.1 mM ANP and 1 μg/mL DT-D, (iii) 0.1 mM ANP and 1.0 mM NADH, and (iv) 0.1 mM ANP, 1.0 mM NADH, and 1 μg/mL DT-D after an incubation period of 10 min at 25 °C. (c) Histogram of signal-to-background ratios for three potential substrates. The signal and background values were calculated from the charge values measured at 100 s in the chronocoulograms obtained at 0.10 V at bare ITO electrodes in tris buffer (pH 9.5) containing (i) 0.1 mM substrate and 1.0 mM NADH, and (ii) 0.1 mM substrate, 1.0 mM NADH, and 1 μg/mL enzyme (DT-D or ALP) after an incubation period of 10 min at 25 °C. (d) Cyclic voltammograms obtained (at a scan rate of 20 mV/s) at bare ITO electrodes in tris buffer (pH 9.5) containing (i) 0.1 mM AN, (ii) 0.1 mM AN and 1.0 mM NADH, and (iii) 0.1 mM AN, 1.0 mM NADH, and 1 μg/mL DT-D after an incubation period of 10 min at 25 °C.

currents are low and reproducible at ITO electrodes. Therefore, the ITO electrode was chosen as a working electrode that allows a low and reproducible background level.

Three phosphate group-containing compounds (APP, AAP, and ANP) were tested as possible substrates (Figure 1a). APP and AAP are widely used as substrates of ALP,[20,31,32] and ANP was recently developed as a substrate of ALP.[33] The three compounds are electrochemically inactive, but the dephosphorylated compounds are readily electrochemically oxidized near 0 V. Figure 3a shows cyclic voltammograms obtained in the absence and presence of DT-D in tris buffer (pH 9.5) containing ANP and NADH after an incubation period of 10 min. In the presence of DT-D, the anodic currents were significantly increased because of the generation of the dephosphorylated product. However, in the cases of APP and AAP, the anodic currents changed slightly (Figure S-1 in the Supporting Information). These results indicate that the dephosphorylation of APP and AAP by DT-D was slow, but that of ANP was very fast. It shows that the rate of reductive phosphorylation was highly dependent on the type of substrate.

To further investigate the dephosphorylation of ANP by DT-D, chronocoulograms were obtained (Figure 3b). The slope in the chronocoulogram obtained in the presence of ANP (curve i of Figure 3b) and the slope obtained in the presence of ANP and DT-D (curve ii of Figure 3b) were low. This indicates that the dephosphorylation of ANP did not occur or was very slow in the presence of only DT-D. The slope obtained in the presence of ANP and NADH (curve iii of Figure 3b) was also low. The slope obtained in the presence of ANP, NADH, and DT-D (curve iv of Figure 3b) was very high, indicating that DT-D and NADH are required for the dephosphorylation. The high slope was obtained because (i) the dephosphorylation by DT-D is fast, (ii) the electrochemical oxidation of AN is fast even at the bare ITO electrode, and (iii) the redox cycling involving AN is fast.

Chronocoulograms for APP and AAP were also obtained in the presence of NADH and in the presence of NADH and DT-D. For comparison, a histogram for the charge data measured at 100 s in the chronocoulograms was drawn (Figure 3c). The background level corresponds to the charge value obtained in the presence of substrate and NADH, whereas the signal level corresponds to that obtained in the presence of substrate, NADH, and DT-D. The signal-to-background (S/B) ratio was 1.2, 2.3, and 15.0 for APP, AAP, and ANP, respectively. ANP showed much higher S/B ratio than APP and AAP. Therefore, ANP was used as a substrate of DT-D for further experiments. For further comparison, chronocoulograms for ANP in the presence of NADH and in the presence of NADH and ALP were obtained. The S/B ratio for ANP and ALP was 5.1 (Figure 3c), which was lower than the value (15.0) for ANP and DT-D. Although ALP rapidly converts ANP to AN, AN participates in one redox cycling scheme: the EC redox cycling involving ITO electrode, AN, and NADH. As ALP is not a


DOI: 10.1021/acs.analchem.9b00064
Anal. Chem. XXXX, XXX, XXX−XXX

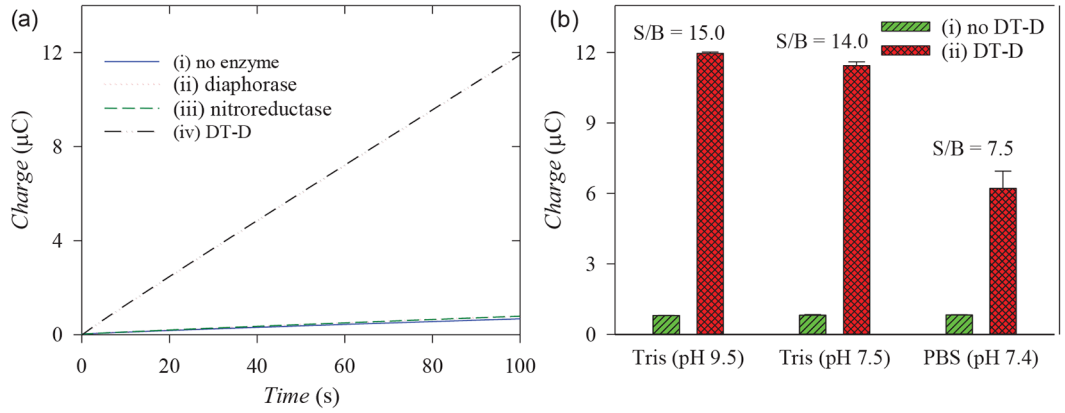


**Figure 4.** (a) Chronocoulograms obtained at 0.10 V at bare ITO electrodes in tris buffer (pH 9.5) containing 0.1 mM ANP, 1.0 mM NADH, and an enzyme: (i) no enzyme, (ii) 1 $\mu$g/mL diaphorase, (iii) 1 $\mu$g/mL nitroreductase, and (iv) 1 $\mu$g/mL DT-D after an incubation period of 10 min at 25 °C. (b) Histogram of signal-to-background ratios calculated from the charge values measured at 100 s in the chronocoulograms obtained at 0.10 V at bare ITO electrodes in three different buffer solutions containing (i) 0.1 mM ANP and 1.0 mM NADH and (ii) 0.1 mM ANP, 1.0 mM NADH, and 1 $\mu$g/mL DT-D after an incubation period of 10 min at 25 °C.

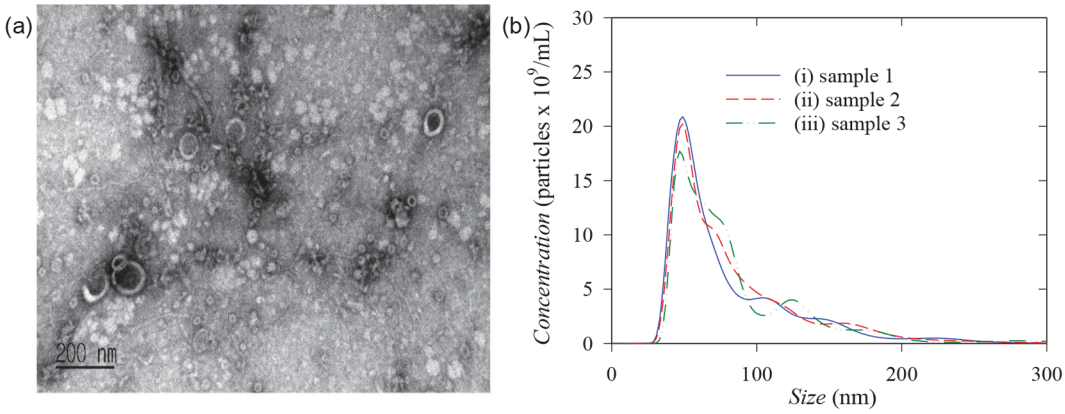


**Figure 5.** (a) TEM image of OMVs isolated from *E. coli* BW 25113 strain. (b) Size distribution of OMVs obtained using NTA.

redox enzyme, EN redox cycling cannot occur. In the case of DT-D, AN participates in two redox cycling schemes (Figure 1b): the EC redox cycling involving ITO electrode, AN, and NADH and the EN redox cycling involving ITO electrode, AN, DT-D, and NADH. These two redox cycling processes contribute to the high electrochemical signal.

To investigate the relative contribution of the EC and EN redox cycling to the electrochemical signal, cyclic voltammograms were obtained in three different solutions (Figure 3d). The currents obtained at potentials higher than 0.0 V during the anodic scan in the presence of AN and NADH (curve ii of Figure 3d) were slightly higher than those obtained in the presence of only AN (curve i of Figure 3d). However, the currents obtained in the presence of AN, NADH, and DT-D (curve iii of Figure 3d) were much higher. The results indicate that the EN redox cycling is much faster than the EC redox cycling. It is interesting to note that the currents negatively increased at potentials lower than −0.1 V during the cathodic scan in the presence of AN alone (curve i of Figure 3d). The cathodic currents are due to AN-mediated oxygen reduction (EC redox cycling involving ITO electrode, AN, and dissolved oxygen). AN is rapidly oxidized by dissolved oxygen, and the oxidized form of AN is then electrochemically reduced at the ITO electrode. The cathodic currents were much lower in the presence of AN and NADH (curve ii of Figure 3d). This is due to the fact that the oxidized form of AN is rapidly reduced by NADH.

There are many enzymes that can oxidize NADH. Just like DT-D, these enzymes might catalyze reductive dephosphorylation. To check this possibility, dephosphorylation activities of diaphorase (EC 1.8.1.4) and nitroreductase from *E. coli* (N9284) were tested (Figure 4a). When diaphorase was present, the slope in the chronocoulogram (curve ii of Figure 4a) was similar to that obtained in the absence of diaphorase (curve i of Figure 4a). In the case of nitroreductase, no significant charge increase was also observed (curve iii of Figure 4a). However, a high charge increase was observed in the case of DT-D (curve iv of Figure 4a). These results indicate that the dephosphorylation of ANP by DT-D was much faster than that by the tested diaphorase and nitroreductase.

ALP has high catalytic activities in basic pH (pH 9.0−9.6) and low activities in neutral pH values.[34] Therefore, there is a limitation in the use of ALP in neutral solutions. The charge level obtained in the presence of DT-D in a neutral tris buffer (pH 7.5) was similar to that obtained in a basic tris buffer (pH 9.5; Figure 4b). This result indicates that the dephosphorylation of ANP by DT-D is fast even in neutral solutions. As dephosphorylation is a reversible reaction, it might become slow in phosphate-containing solutions. In PBS (pH 7.4),


DOI: 10.1021/acs.analchem.9b00064
Anal. Chem. XXXX, XXX, XXX−XXX

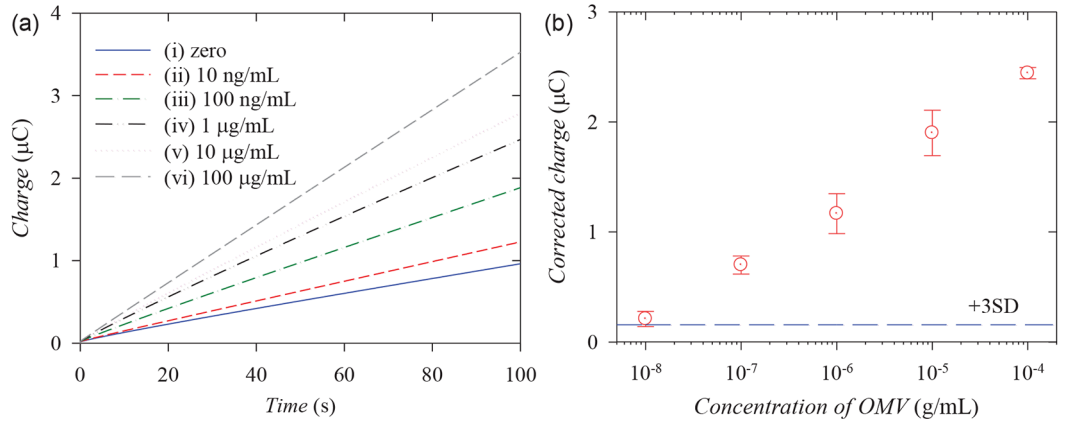


**Figure 6.** (a) Chronocoulograms obtained at 0.10 V at immunosensing electrodes treated with PBS buffer (pH 7.4) containing various concentrations of OMV after an incubation period of 10 min at 25 °C in tris buffer (pH 9.5) containing 0.1 mM ANP and 1.0 mM NADH. (b) Calibration plot for the charge measured at 100 s in the chronocoulograms of panel a. All the charged data were subtracted from the mean value of seven measurements obtained at the zero concentration. The dashed line corresponds to three times the standard deviation at the zero concentration. The error bars represent the standard deviation of three measurements.

phosphorylation was slower than that in tris buffers (Figure 4b). Nevertheless, the phosphorylation was not very slow in PBS.

**OMV Detection.** OMV was extracted from *E. coli* BW25113 strain that was cultured on LB medium. The resulting OMV fraction was also added to the LB medium and cultured, but they were not included in the bacterial growth (data not shown). The isolated OMV was characterized using TEM and NTA (Figure 5). The TEM image shows that the isolated OMV has sizes ranging from 57 to 104 nm (Figure 5a). From NTA, the size of OMV was 88 ± 61 nm (Figure 5b).

A sandwich-type immunosensor was developed to achieve sensitive and specific OMV detection (Figure 1b). As one OMV contains many LPSs, one OMV can bind more than two identical anti-LPS IgGs. Therefore, two anti-LPS IgGs were used as two sandwich probes. The multiple binding sites might allow fast affinity binding between OMV and anti-LPS IgGs. The OMVs present in the PBS or LB medium were first captured on the sensing electrode immobilized with biotinylated anti-LPS IgG. DT-D-conjugated anti-LPS IgG was then attached to the captured OMV. Unbound DT-D-conjugated IgG was washed away. During an incubation period of 10 min, DT-D converted ANP to AN in the presence of NADH (reaction i of Figure 1b). AN concentration near the electrode significantly increased in the short incubation period. When a potential of 0.1 V was applied to the electrode, AN was electrochemically oxidized to naphthoquinone imine (reaction ii of Figure 1b). The imine was then reduced to AN by two reactions: chemical reduction by NADH (reaction iii of Figure 1b) and enzymatic reduction by DT-D and NADH (reaction iv of Figure 1b). The regenerated AN was electrochemically oxidized again at the electrode. As a result, two redox cycling processes occur: the EC redox cycling involving ITO electrode, AN, and NADH (combination of reactions ii and iii of Figure 1b) and the EN redox cycling involving ITO electrode, AN, DT-D, and NADH (combination of reactions ii and iv of Figure 1b). Highly amplified electrochemical signals are due to fast enzymatic amplification by dephosphorylation, fast electrochemical oxidization, fast EC redox cycling, and fast EN redox cycling.

Figure 6a shows chronocoulograms obtained at 0.1 V after carrying out OMV detection in various OMV concentrations. The slope in the chronocoulograms increased with increasing OMV concentrations in PBS. Figure 6b shows a calibration plot obtained using the charge values measured at 100 s in the chronocoulograms. The calculated detection limit for OMV was approximately 8 ng/mL, which indicated that the immunosensor for OMV detection is sensitive. To confirm the accuracy of the developed immunosensor, the concentrations of OMV in three LB media as real samples were measured. The concentrations measured using BCA protein assay kit were 7.5, 3.0, and 4.1 μg/mL, whereas the concentrations measured using the developed immunosensor were 10.0, 3.0, and 3.9 μg/mL. The two corresponding values were in a good agreement.

## CONCLUSIONS

We found that DT-D catalyzes rapid reductive dephosphorylation of a phosphate-containing substrate (particularly, ANP) in the presence of NADH. This catalytic activity was applied to sensitive and simple detection of Gram-negative bacterial OMVs containing pyrogenic LPSs. For this purpose, a sandwich-type electrochemical immunosensor was developed using DT-D and two identical anti-LPS IgGs as a catalytic label and two sandwich probes, respectively. High electrochemical signals were obtained due to (i) the fast reductive dephosphorylation of ANP by DT-D, (ii) the rapid electrochemical oxidation of AN at an ITO electrode, and (iii) the fast EN and EC redox cycling involving AN. The electrochemical signals even in neutral buffers were comparable to the signals in basic buffers (tris buffer, pH 9.5). When the immunosensor was applied to the detection of OMV from *E. coli*, the detection limit was 8 ng/mL. The detection strategy is highly promising for the detection of biomaterials including other extracellular vesicles.

## ASSOCIATED CONTENT

### Supporting Information

The Supporting Information is available free of charge on the ACS Publications website at DOI: 10.1021/acs.analchem.9b00064.



DOI: 10.1021/acs.analchem.9b00064
*Anal. Chem.* XXXX, XXX, XXX−XXX

Cyclic voltammograms of two potential substrates (PDF)

## AUTHOR INFORMATION


### Corresponding Authors

*E-mail: hyang@pusan.ac.kr.

*E-mail: kwangsun.kim@pusan.ac.kr. Fax: (+82)-51-516-7421.

### ORCID

Jung Min Joo: 0000-0003-1645-3322

Haesik Yang: 0000-0001-7450-5915


### Notes

The authors declare no competing financial interest.

## ACKNOWLEDGMENTS

This research was supported by the National Research Foundation of Korea (2018R1A2B2004122, 2017M3A7B4041973, and 2016M3A7B4910538). This research is also supported by the Ministry of Trade, Industry, and Energy (MOTIE, Korea) under the Industrial Technology Innovation Program (No. 10062995).

## REFERENCES


(1) Anand, D.; Chaudhuri, A. *Mol. Membr. Biol.* **2016**, *33*, 125−137.

(2) Schwechheimer, C.; Kuehn, M. *Nat. Rev. Microbiol.* **2015**, *13*, 605−619.

(3) Horstman, A. L.; Kuehn, J. M. *J. Biol. Chem.* **2000**, *275*, 12489−12496.

(4) Ellis, T. N.; Kuehn, J. M. *Microbiol. Mol. Biol. Rev.* **2010**, *74*, 81−94.

(5) Ding, X.; Su, W. *J. Laboratory Automation.* **2015**, *20*, 354−364.

(6) Gutsmann, T.; Schromm, A. B.; Brandenburg, K. *Int. J. Med. Microbiol.* **2007**, *297*, 341−352.

(7) Kulp, A.; Kuehn, M. J. *Annu. Rev. Microbiol.* **2010**, *64*, 163−184.

(8) Parija, S. C. *Textbook of Microbiology and Immunology*; Elsevier: India, 2009.

(9) Santos, J. C.; Dick, M. S.; Lagrange, B.; Degrandi, D.; Pfeffer, K.; Yamamoto, M.; Meunief, E.; Pelczar, P.; Henry, T.; Broz, P. *EMBO J.* **2018**, *37*, No. e98089.

(10) Vanaja, S. K.; Russo, A. J.; Behl, B.; Banerjee, I.; Yankova, M.; Deshmukh, S. D.; Rathinam, A. K. *Cell* **2016**, *165*, 1106−1119.

(11) Gamalier, J. P.; Silva, T. P.; Zarantonello, V.; Dias, F. F.; Melo, R. C. N. *Microbiol. Res.* **2017**, *194*, 38−46.

(12) Miao, P. *RSC Adv.* **2013**, *3*, 9606.

(13) Yeo, T. Y.; Choi, J. S.; Lee, B. K.; Kim, S. B.; Yoon, H. I.; Lee, H. Y.; Cho, Y. W. *Biosens. Bioelectron.* **2011**, *28*, 139−145.

(14) Dullah, E. C.; Ongkudon, C. M. *Crit. Rev. Biotechnol.* **2017**, *37*, 251−261.

(15) Das, A. P.; Kumar, P. S.; Swain, S. *Biosens. Bioelectron.* **2014**, *51*, 62−75.

(16) Eissa, S.; Ahmady, O. E. *Protein Phosphorylation and Dephosphorylation: A Mechanism of Acute and Reversible Regulation of Protein Function*; LAP Lambert Academic Publishing: Saarbrucken, Germany, 2012.

(17) Carlson, C. A.; Kim, K. H. *J. Biol. Chem.* **1972**, *248*, 378−380.

(18) Ardito, F.; Giuliani, M.; Perrone, D.; Troiano, G.; Muzio, L. L. *Int. J. Mol. Med.* **2017**, *40*, 271−280.

(19) Aziz, M. A.; Jo, K.; Qaium, M. A.; Huh, C. H.; Hong, I. S.; Yang, H. *Electroanalysis* **2009**, *21*, 2160−2164.

(20) Akanda, R. M.; Aziz, M. A.; Jo, K.; Tamilavan, V.; Hyun, M. H.; Kim, S.; Yang, H. *Anal. Chem.* **2011**, *83*, 3926−3933.

(21) Yang, H. *Curr. Opin. Chem. Biol.* **2012**, *16*, 422−428.

(22) Kemp, B. E.; Froscio, M.; Murray, A. W. *Biochem. J.* **1973**, *131*, 271−274.

(23) Allison, W. S.; Benitez, L. V. *Proc. Natl. Acad. Sci. U. S. A.* **1972**, *69*, 3004−3008.

(24) Polgár, L. *Experientia* **1964**, *20*, 408−413.

(25) Wilson, M. S.; Rauh, R. D. *Biosens. Bioelectron.* **2004**, *20*, 276−283.

(26) Lee, W. H.; Choi, H. I.; Hong, S. W.; Kim, K. S.; Gho, Y. S.; Jeon, S. G. *Exp. Mol. Med.* **2015**, *47*, No. e183.

(27) Gardiner, C.; Ferreira, Y. J.; Dragovic, R. A.; Redman, C. W. G.; Sargent, I. L. *J. Extracell. Vesicles* **2013**, *2*, 1−11.

(28) Choi, M.; Jo, K.; Yang, H. *Bull. Korean Chem. Soc.* **2013**, *34*, 421−425.

(29) Rover, L., Jr.; Fernandes, J. C. B.; Neto, G. de O.; Kubota, L. T.; Katekawa, E.; Serrano, S. H. P. *Anal. Biochem.* **1998**, *260*, 50−55.

(30) Kang, C.; Kang, J.; Lee, N.; Yoon, Y. H.; Yang, H. *Anal. Chem.* **2017**, *89*, 7974−7980.

(31) Das, J.; Jo, K.; Lee, J. W.; Yang, H. *Anal. Chem.* **2007**, *79*, 2790−2796.

(32) Preechaworapun, A.; Dai, Z.; Xiang, Y.; Chailapakul, O.; Wang, J. *Talanta* **2008**, *76*, 424−431.

(33) Seo, J.; Ha, H.; Park, S.; Haque, A. M. J.; Kim, S.; Joo, J. M.; Yang, H. *ACS Sens* **2017**, *2*, 1240−1246.

(34) Savage, M. D. *Avidin-Biotin Chemistry: A Handbook*; Pierce Chemical Company: Rockford, IL, 1992.




DOI: 10.1021/acs.analchem.9b00064
*Anal. Chem.* XXXX, XXX, XXX−XXX